CONF-790441--7

# IODINE STRESS-CORROSION CRACKING IN IRRADIATED ZIRCALOY CLADDING

by

R.F. Mattas, F.L. Yaggee, and L.A. Neimark



Prepared for

American Nuclear Society Topical Meeting

on

Light Water Reactor Fuel

Portland, Oregon

April 30, 1979 - May 2, 1979



U of C-AUA-USDOE

ARGONNE NATIONAL LABORATORY, ARGONNE, ILLINOIS

Operated under Contract W-31-109-Eng-38 for the

U. S. DEPARTMENT OF ENERGY

## DISCLAIMER

The facilities of Argonne National Laboratory are owned by the United States Government. Under the terms of a contract (W-31-109-Eng-38) among the U. S. Department of Energy, Argonne Universities Association and The University of Chicago, the University employs the staff and operates the Laboratory in accordance with policies and programs formulated, approved and reviewed by the Association.

MEMBERS OF ARGONNE UNIVERSITIES ASSOCIATION

| | | |
|---|---|---|
| The University of Arizona | Kansas State University | The Ohio State University |
| Carnegie-Mellon University | The University of Kansas | Ohio University |
| Case Western Reserve University | Loyola University | The Pennsylvania State University |
| The University of Chicago | Marquette University | Purdue University |
| University of Cincinnati | Michigan State University | Saint Louis University |
| Illinois Institute of Technology | The University of Michigan | Southern Illinois University |
| University of Illinois | University of Minnesota | The University of Texas at Austin |
| Indiana University | University of Missouri | Washington University |
| Iowa State University | Northwestern University | Wayne State University |
| The University of Iowa | University of Notre Dame | The University of Wisconsin |

# IODINE STRESS-CORROSION CRACKING IN IRRADIATED ZIRCALOY CLADDING

R. F. Mattas, F. L. Yaggee, and L. A. Neimark

Argonne National Laboratory
Argonne, Illinois 60439, U.S.A.

## ABSTRACT

Irradiated Zircaloy cladding specimens, which had experienced fluences from 0.1 to 6 x $10^{21}$ n/cm$^2$ (E>0.1 MeV), were gas-pressure tested in an iodine environment to investigate their stress-corrosion cracking (SCC) susceptibility. The test temperatures and hoop stresses ranged from 320 to 360°C and 150 to 500 MPa, respectively. The results indicate that irradiation, in general, increases the susceptibility of Zircaloy to iodine SCC. For specimens that experienced fluences $\geq 2 \times 10^{21}$ n/cm$^2$ (E>0.1 MeV), the 24-h failure stress was $177 \pm 18$ MPa, regardless of the preirradiation metallurgical condition. An analytical model for iodine SCC has been developed which agrees reasonably well with the test results.

## INTRODUCTION

Pellet-cladding interaction (PCI) has been identified as a cause of fuel-rod failures in commercial reactors. The failures are usually tight cracks that exhibit little or no plastic deformation.(1) They are usually located at pellet-pellet interfaces, often adjacent to fuel-pellet cracks. The fracture surfaces of the cracks consist predominantly of cleavage planes with a small percentage of ductile fluting. PCI failures are similar in appearance to failures due to stress-corrosion cracking (SCC).(2) The corrodant species is believed to be a fission product generated during irradiation. Rosenbaum, et al. have shown that the fission-product iodine produces SCC fractures which closely resemble PCI failures.(3) More recently, it was shown that failures in Zircaloy specimens in either cadmium or cesium environments also closely resemble PCI failures.(4) However, iodine remains a likely candidate for the fission product responsible for PCI failures.

The present investigation was undertaken to determine the susceptibility of irradiated Zircaloy cladding to iodine SCC. Several cladding sources were used in the investigation and both PWR and BWR cladding specimens were tested. The specimens were subjected to short-term (<100-h) biaxial gas-pressurization tests in an iodine environment. The important parameters in these tests are temperature, hoop stress, and time to failure. The cladding and the SCC failures were characterized by scanning electron microscopy and optical metallography.

## EXPERIMENTAL PROCEDURES

The cladding used in this investigation came from a number of sources. Irradiated Zircaloy-2 cladding came from fuel rods from the Oskarshamn-1 (OSK-1), Quad Cities-1 (QC), and Big Rock Point (BRP) reactors, while Zircaloy-4 cladding came from fuel rods from the H. B. Robinson (HBR) reactor. A summary of the cladding characteristics is shown in Table I. The irradiated OSK-1 specimens were obtained from both failed and unfailed fuel rods[5] that had been involved in a preplanned control-rod withdrawal. All other cladding experienced normal reactor operating conditions, and came from unfailed fuel rods.

The nominal specimen length used in the SCC tests was 15 cm. Prior to testing, the fuel was removed, and a two-piece Vycor volume-displacement slug was inserted. The Vycor slug displaced ∿98% of the specimen volume to minimize the quantity of high-pressure gas in the system. If the specimen was to be tested with iodine, a Vycor ampule containing 25 mg of iodine was also inserted. Just prior to sealing the specimen, the Vycor ampule was crushed to release the iodine. The ends of the specimen were sealed with modified Swagelok fittings. Figure 1 shows the configuration of the assembled specimen. The iodine SCC tests were performed in-cell using a biaxial creep apparatus which has been described elsewhere.[6] With few exceptions, the iodine SCC tests were conducted under "short" volume conditions where the total system volume, including the specimen, was ∿85 $cm^3$. The system pressure was controlled to within 2% and was recorded continuously. The pressurizing gas was either helium or argon. The temperature of the specimen was controlled to ±1°C and was also recorded continuously.

An SCC test consisted of heating a sealed specimen to the desired test temperature and then pressurizing it to the desired hoop stress. The temperature and pressure were normally held at constant values until the specimen failed. During initial tests where the low-stress region of the stress vs time to failure curve was unknown, the SCC tests were run in time-pressure increments. These SCC tests were run at a constant stress for a period of 10-24 h. If specimen failure did not occur, the stress level was raised and held for an additional 10-24 h period. The stress level was repeatedly raised in this manner until failure occurred during a 10-24 h period. Once the region of the lower-threshold stress was approximately established in this manner, longer-time tests were conducted to better define the threshold. The tests were conducted at temperatures from 320 to 360°C and at stresses from 150 to 500 MPa. Iodine concentrations of ∿0.6 and 6.0 $mg/cm^2$ were used.

Optical metallography and scanning electron microscopy (SEM) were used to characterize the cladding and SCC failures. Metallographic and SEM specimens were cut dry from the cladding using a high-speed (1000 rpm) alumina cutoff wheel. The metallographic specimens were mounted transversely and were examined in both the as-polished and etched conditions. The etching solution, consisting of 46% $H_2O$, 46% $HNO_3$, and 8% HF was used to reveal the hydride structure. The SEM examination of the SCC failures consisted of examination

and photography of the SCC crack on the ID surface, ultrasonic cleaning of the ID surface, and reexamination of the cleaned crack. The crack was then split open by three-point bending, and the entire fracture surface was examined.

## RESULTS

Table II compares the ID oxide, OD oxide, and hydride characteristics of the different claddings. With the exception of the low-burnup ( $1 \times 10^{21}$ $n/cm^2$) BRP cladding, all specimens exhibited thin or nonuniform ID oxide layers. In the case of the high-burnup ( $4 \times 10^{21}$ $n/cm^2$) BRP cladding, the ID oxide reached a thickness of up to 18 μm in some areas, while it could not be detected in other areas. The low-burnup BRP cladding was unique in that the ID oxide had a uniform thickness of 3-4 μm around the circumference. The OD oxide of the OSK-1 and QC claddings was nodular and penetrated 20-40 μm into the cladding at the nodules. These nodules could easily be removed to reveal the underlying Zircaloy substrate. Nodules were not present on the other claddings. The thin regions of OD oxide found on all BWR claddings ranged in thickness from 0.5 to 3 μm. The OD oxide on the HBR cladding ranged in thickness from 20 to 25 μm. The hydride content of the claddings was generally low.

The results of the SCC pressurization tests are shown in Figs. 2 to 5. The curves shown in Figs. 2-5 were fitted to the data by the SCC model discussed below. The results of the OSK-1 tests, shown in Fig. 2, compare the times to failure for specimens tested with and without iodine at 344°C. The effect of iodine is to markedly reduce the stress required for a given time to failure. The stress required to cause failure in 24 h ($8.6 \times 10^4$ s) drops from ~425 MPa to 160 MPa with the addition of iodine. The fact that the OSK-1 specimens came from both failed and unfailed fuel rods does not appear to affect the stress vs time to failure curve. Figure 3 shows the results of tests at 325°C on QC specimens. The stress required to induce failure in 24 h is ~180 MPa, close to that of the OSK-1 cladding, but the times to failure at high stress levels are a factor of 2.5-3 greater than those of the OSK-1 cladding. Figure 4 compares the times to failure of HBR cladding tested at 360° and 325°C. The complete curve at 360°C indicates that the 24-h failure stress is ~195 MPa. The effect of temperature is apparent at the higher stress of 412 MPa, where the failure time is increased by a factor of ~10 when the test temperature is reduced from 360° to 325°C. The dotted line in Fig. 4 is the SCC-model prediction for the 325°C tests. Two iodine concentrations, 0.6 and 6.0 $mg/cm^2$, were employed in the HBR tests. No detectable differences in the SCC behavior were observed, indicating that both concentrations are above the saturation level for the effect of iodine on SCC. Figure 5 compares the results for BRP cladding at three different fuel-rod burnups. The cladding from the high-burnup BRP rod exhibits times to failure similar to those of the QC cladding tested at the same temperature. The limited data indicate that the cladding from the low-burnup BRP rod is as resistant to SCC as the short-cycle cladding, even though it experienced a considerably greater fluence. The low-stress portions of the time-to-failure curves for all claddings appear to have a shallow downward slope. For comparative purposes, a summary of the 24-h failure stresses is shown in Table III. These stresses are representative of the flat or "threshold" portions of the stress vs time to failure curves.

Optical metallography and scanning electron microscopy were used to characterize the failures. Figure 6 shows an etched section of a failed high-burnup BRP specimen, tested at 172 MPa. This cladding shows multiple crack-initiation sites. All of the cracks are tight, and there is no indication of gross plastic deformation. Hydrides are generally observed along and ahead of the cracks. Figure 7 shows the appearance of an SCC failure in a QC specimen,

tested at 182 MPa. Figure 7a shows the crack along the ID surface in the as-tested condition. The crack is ∿1 cm long and is partially covered by a corrosion product. X-ray analysis of the corrosion product indicates a large concentration of Zirconium and a small concentration of iodine. Ultrasonic cleaning removed the corrosion product to reveal a high degree of chemical attack near the middle of the crack (Fig. 7b). The crack was split open by three-point bending to reveal the fracture surface (Fig. 7c). The corrosion product is apparent near the center of the fracture. In general, the crack length-to-depth ratio is ∿10, and the curved crack front leads to a pinhole penetration at the OD surface. Figure 8 compares the fracture surfaces of QC specimens tested at 182 and 412 MPa. The low-stress failure exhibits the cleavage and fluting features thought to be typical of iodine SCC in Zircaloy, whereas the high-stress failure exhibits an atypical fracture surface.

## DISCUSSION

### Effect of Cladding Characteristics on Iodine SCC

The cladding materials used in this investigation experienced fluences ranging from 0.1 to 6 x $10^{21}$ n/cm$^2$ (E>0.1 MeV). The results indicate that those materials (OSK-1, QC, HBR, and high-burnup BRP) which received a fluence of greater than 2 x $10^{21}$ n/cm$^2$ exhibited similar stress-corrosion behavior. The preirradiation heat treatment of the cladding did not appear to affect the test results. The change in mechanical properties of Zircaloy with irradiation is known to reach a saturation level at a fluence of 2-4 x $10^{20}$ n/cm$^2$ regardless of initial heat treatment[7]; the susceptibility of Zircaloy to iodine SCC also appears to reach a saturation level at ∿2 x $10^{20}$ n/cm$^2$.[8] The similarity among these claddings with respect to iodine SCC and the reduced susceptibility of the short-cycle BRP cladding is consistent with the changes in Zircaloy mechanical properties with fluence. The implication is that the cladding mechanical properties influence the stress-corrosion behavior of Zircaloy.

The exception to this argument is the low-burnup BRP cladding. This cladding received a fluence of 0.6 to 1 x $10^{21}$ n/cm$^2$ (E> 0.1 MeV), which is above the saturation level for changes in mechanical properties. On the basis of the above discussion, this cladding would be expected to show SCC behavior similar to that of claddings that received a higher fluence. One feature of this cladding which may influence SCC susceptibility is the uniformly thick oxide layer on the ID surface. Such an oxide layer could inhibit iodine SCC in two ways. Presumably, crack initiation requires iodine penetration of the oxide to the Zircaloy substrate, and a thick oxide layer is likely to provide a barrier to iodine attack. Second, a thick oxide layer is likely to result in a compressive stress on the ID surface because of the volume increase that accompanies oxide formation.[9] The compressive stress would have to be overcome before the oxide could crack and SCC could take place. Residual stresses in the Zircaloy substrate have been shown to have a significant effect on iodine SCC in unirradiated Zircaloy.[8]

Other cladding characteristics, such as the OD oxide and hydride content, do not appear to be directly correlated with the SCC behavior of the irradiated claddings.

## SCC Model

The results described in the preceding sections have been integrated into an analytical model to describe iodine SCC in Zircaloy. The model is based on the observation that iodine SCC failures usually begin as an intergranular fracture which becomes a "cleavage and fluting" fracture at some point in crack growth. It is assumed in the model that the intergranular portion of the failure is due to chemical attack which is independent of applied stress, while the cleavage and fluting portion of the failure can be described by linear elastic fracture mechanics. The time to failure, $t_f$, in an SCC test can thus be divided into the time $t_{ch}$ required to chemically grow an intergranular crack and the time $t_{cf}$ required to propagate the crack to failure by cleavage and fluting; i.e.,

$$t_f = t_{ch} + t_{cf} \tag{1}$$

The chemical crack-growth rate $\dot{a}$ is assumed to have an initial value $A_o$, and to decrease exponentially as the crack depth increases:

$$\dot{a} = A_o \exp(-a/B) \tag{2}$$

where a is the crack depth and B is a rate constant. Chemical crack growth is assumed to continue until a critical stress intensity for cleavage and fluting, $K_{ISCC}$, is reached. At this point, cleavage and fluting fracture initiates and continues to failure. The derived times to failure are

$$t_{ch} = \frac{B}{A_o}\left[\exp\left(\frac{K_{ISCC}^2}{y^2\sigma^2 B}\right) - 1\right] \tag{3}$$

and

$$t_{cf} = \frac{C}{\sigma^4 y^4}\left[\frac{\sigma^2 y^2}{K_{ISCC}^2} - \frac{\sigma_B}{W(\sigma_B-\sigma)}\right] \tag{4}$$

where y is a geometric factor $\approx 2$,[10] $\sigma$ is the applied hoop stress, C is a rate constant, $\sigma_B$ is the hoop burst stress, and W is the cladding wall thickness. The derivation of Eq. (4) is based upon the cladding crack analysis of Kreyns et al.[10] Equations 3 and 4 are valid for high-strength cladding where $K_{ISCC}$ is reached before stress-rupture conditions are achieved. When stress-rupture conditions are reached before $K_{ISCC}$, e.g., in unirradiated annealed cladding, the time to failure is

$$t_f = \frac{B}{A_o}\left[\exp\left(\frac{W(\sigma_B-\sigma)}{\sigma_B B}\right) - 1\right] \tag{5}$$

The details of the above derivations are given elsewhere.[11]

The parameters $\sigma_B$, $K_{ISCC}$, and y have been estimated from the literature,[10,12,13] while the remaining parameters $A_o$, B, and C have been evaluated by fitting Eqs. (3) and (4) to the OSK-1 and QC data. A summary of the parameters used for the two types of cladding is given in Table IV. The differences in the two sets of data can be accounted for by the changes in just two parameters, $A_o$ and C. The principal difference between the test conditions for the OSK-1 and QC data is the temperature. Assuming that the differences in $A_o$ and C are due to the different test temperatures, apparent activation

energies for these terms can be calculated by assuming that both $A_o$ and C obey Arrhenius equations

$$A_o = A_1 \exp(-\Delta H_1/RT);$$
$$C = C_1 \exp(+\Delta H_2/RT) . \quad (6)$$

The values $A_1$, $\Delta H_1$, C1, and $\Delta H_2$ thus estimated from the data are

$$A_1 = 3.55 \times 10^{10} \text{ m/n}, \Delta H_1 = 40 \text{ kcal/mole}$$
$$C_1 = 1.15 \times 10^{-3} \text{ MPa}^4\text{-m-h}, \Delta H_2 = 28 \text{ kcal/mole} .$$

In the model, it is assumed that the threshold stress intensity, $K_{ISCC}$, varies with the yield strength of Zircaloy. Decreases in $K_{ISCC}$ with increased yield strength have been observed in steels, titanium alloys, and aluminum alloys in other environments[14-16] and have been theoretically predicted to be a general characteristic of SCC.[17] However, $K_{ISCC}$ has not been directly measured as a function of the mechanical properties of Zircaloy, and, therefore, it is not known what, if any, change in $K_{ISCC}$ will occur. Theoretical arguments by Smith et al. predict little difference in $K_{ISCC}$ between unirradiated and irradiated Zircaloy.[18] The observed value of $K_{ISCC}$ in stress-relieved Zircaloy is 9-10 MPa-$m^{\frac{1}{2}}$.[19] This $K_{ISCC}$ value was determined using compact-tension fracture-mechanics specimens which were wedge-opening loaded under plain-strain conditions. In the absence of test data, it will be assumed that $K_{ISCC}$ decreases linearly with yield strength.

$$K_{ISCC} = K_o - K_1 * \sigma_{ys} \quad (7)$$

where $K_o$ = 24.5 MPa-$m^{\frac{1}{2}}$, $K_1 = 3.25 \times 10^{-2}$ $m^{\frac{1}{2}}$, and $\sigma_{ys}$ is the hoop yield stress. Equation (7) predicts a $K_{ISCC}$ of 10 MPa-$m^{\frac{1}{2}}$ for $\sigma_{ys} \cong 446$ MPa (65 ksi) and a $K_{ISCC}$ of 4.5 MPa-$m^{\frac{1}{2}}$ for $\sigma_{ys}$ = 615 MPa (89 ksi).

The effect of cladding mechanical properties on the model predictions is compared in Fig. 9 with data from SCC tests of both unirradiated and irradiated cladding. The unirradiated test data were obtained at the Stanford Research Institute for both annealed and stress-relieved cladding at 317°C,[19] and the irradiated test data are the QC data taken at 325°C. Figure 9 indicates that the model predictions agree reasonably well with the test data. The agreement between the model and the test data indicates that the changes in the cladding mechanical properties alone could account for the changes in SCC susceptibility.

Busby et al. have also conducted gas-pressurization tests on unirradiated cladding in the presence of iodine.[20] Quantitative comparisons of the SCC model with their data have not been made at this time because of the lower iodine concentration used in their tests. Qualitatively, however, the data conform to the sigmoidal stress vs time to failure curves predicted by both the present model and that of Kreyns et al.[10] At long times to failure (>1000 h), the data show a threshold stress of ∿140 MPa below which failure does not occur. The value of the apparent "threshold" stress appears to be about the same for both annealed and cold-worked, stress-relieved materials and shows no significant change with temperature in the range studied (360 to 400°C). This threshold stress is not predicted by the model. The reasons for this difference are not known at present.

## CONCLUSIONS

(1) Irradiation, in general, increases the susceptibility of Zircaloy to iodine-induced SCC failures.

(2) A uniformly thick (3-4 μm) oxide layer on the ID of the low-burnup BRP cladding may be responsible for its reduced SCC susceptibility.

(3) The stress required to induce failure within 24 hours in Zircaloy cladding irradiated to above $2 \times 10^{21}$ n/cm$^2$ is 177±18 MPa (26±2.6 ksi).

(4) The preirradiation metallurgical condition of the cladding appears to have little effect on stress vs time to failure in cladding irradiated above the saturation fluence.

(5) An analytical model of iodine SCC has been developed which incorporates a temperature and mechanical-property dependence into the stress-corrosion susceptibility of Zircaloy.

## REFERENCES


(1) N. Fuhrman et al., "Evaluation of Fuel Performance in Main Yankee Core I - Task C," EPRI NP-218 (1976).

(2) B. Cox, J. C. Wood, "Iodine Induced Cracking of Zircaloy Fuel Cladding--A Review," Corrosion Problems in Energy Conversion and Generation, 298 (1974).

(3) H. S. Rosenbaum, Electrochem. Technol. 4, 153 (1966).

(4) W. T. Grubb and M. H. Morgan III, "Cadmium Embrittlement of Zircaloy-2," Proc. ANS Topical Meeting on Water Reactor Fuel Performance, 295 (1977).

(5) V. Pasupathi et al., "Determination and Microscopic Study of Incipient Defects in Irradiated Power Reactor Fuel Rods," EPRI NP-812 (1978).

(6) F. L. Yaggee and R. C. Haglund, "In-Cell Facility for Performing Mechanical Property Tests on Irradiated Cladding," Proc. Conf. on Remote Systems Technology 26, 11 (1979).

(7) "MATPRO-Version 10, A Handbook of Materials Properties for Use in the Analysis of Light Water Fuel Rod Behavior," EG&G, TREE-NUREG-1180 (1978).

(8) J. C. Wood, J. Nucl. Mater. 45, 105 (1972-73).

(9) D. H. Bradhurst and P. M. Heuer, J. Nucl. Mater. 37, 35 (1970).

(10) P. H. Kreyns, G. L. Spahr, and J. E. McCauley, J. Nucl. Mater. 61, 203 (1976).

(11) F. L. Yaggee, R. F. Mattas, and L. A. Neimark, "Interim Report on the Characterization of Irradiated Zircaloys: Susceptibility to Stress-Corrosion Cracking," EPRI report, to be published.

(12) A. A. Bauer, W. J. Gallagher, L. M. Lowry, and A. J. Markworth, "Evaluating Strength and Ductility of Irradiated Zircaloy," BMI-NUREG-1985 (1977).

(13) E. Smith, "Fracture of Zircaloy Cladding by Interactions with Uranium Dioxide Pellets in Water Reactor Fuel Rods," Zirconium in the Nuclear Industry, ASTM STP 633, 543 (1977).

(14) M. O. Speidel, "Current Understanding of Stress Corrosion Crack Growth in Aluminum Alloys," The Theory of Stress Corrosion Cracking in Alloys, ed. J. C. Scully, 289 (Belgium North Atlantic Treaty Organization, Scientific Arrairs Division, 1971).

(15) B. F. Brown, "The Application of Fracture Mechanics to Stress-Corrosion Cracking," Metall. Rev. 129, 171 (1968).

(16) W. W. Gerberich and Y. T. Chen, Met. Trans. A, 6A, 271 (1975).

(17) R. N. Parkins and J. H. Craig, "Environment Sensitive Crack Growth by Dissolution and Hydrogen Adsorption," Proc. of International Conf. on Mechanisms of Environment Sensitive Cracking of Materials, 32 (1977).

(18) E. Smith and A. K. Miller, to be published in J. Nucl. Mater.

(19) D. Cubicciotti and R. L. Jones, "EPRI-NASA Cooperative Project on Stress Corrosion Cracking of Zircaloys," EPRI-NP-717 (1978).

(20) C. C. Busby, R. P. Tucker and J. E. McCauley, J. Nucl. Mater. 55, 64 (1975).

TABLE I.

Summary of Irradiated Zircaloy Cladding Materials
Used in Iodine Stress-corrosion Tests

| Material | Condition | Reactor | Fuel Burnup (MWd/Kg U) | Fluence[a] ($10^{21}$ n/cm$^2$) | Nominal Dimensions (mm) OD | Wall Thickness[b] | Ovality[c] (mm) |
|---|---|---|---|---|---|---|---|
| Zircaloy-2 | Annealed | OSK-1 | 10-14 | 1.8-2.2 | 11.78<br>12.24 | .85<br>.80 | ∿.02<br>∿.02 |
| Zircaloy-2 | Annealed | QC | 8.5-11 | 1.3-1.6 | 14.30 | .94 | <.01 |
| Zircaloy-2 | CW-SR | BRP | 6-10 | 0.6-1 | 9.66 | .86 | <.01 |
| Zircaloy-2 | CW-SR | BRP | 27-30 | 4 | 14.28 | 1.29 | ∿.03 |
| Zircaloy-2 | CW-SR | BRP | 0.7 | 0.1 | 14.28 | 1.14 | ∿.05 |
| Zircaloy-4 | CW-SR | HBR | 27-30 | 5-6 | 10.70 | .61 | .089-.381 |

[a] >0.1 MeV

[b] Determined from difference between OD and ID measurements.

[c] Determined from profilometry measurements.

TABLE II.

Characterization of Irradiated Cladding

| Source | Oxide Thickness (μm) ID | Oxide Thickness (μm) OD | Hydride Distribution |
|---|---|---|---|
| H. B. Robinson | 0.5-7 | 20-30 (uniform) | circumferential |
| Oskarshamn | 1-4 | 3-40 (nodular) | random |
| Quad Cities | 0.5-6 | 1-40 (nodular) | random |
| Big Rock Point (high burnup) | 0.5-18 | 1-3[a] | random |
| Big Rock Point (low burnup) | 3-4 (uniform) | 103 (uniform) | random |
| Big Rock Point (short cycle) | <0.5 | <0.5 | random |

[a] Plus 50-70 μm of crud.

Table III.

24-hour Failure-stress Values for Irradiated Cladding Materials

| Cladding | Failure Stress (MPa) |
|---|---|
| HBR | 195 |
| OSK-1 | 160 |
| QC | 180 |
| BRP (low-burnup) | 290 |
| BRP (high-burnup) | 165 |
| BRP (short-cycle) | 250 |

Table IV.

Parameters Used in SCC Model

| Parameter | Oskarshamn | Quad Cities |
|---|---|---|
| Test Temperature (°K) | 617 | 598 |
| Iodine Concentration ($mg/cm^2$) | 0.5 | 0.5 |
| Assumed Burst Stress (MPa) | 690[12] | 690[12] |
| $K_{ISCC}$ ($MPa\text{-}m^{\frac{1}{2}}$) | 4.4[13] | 4.4[13] |
| Y | 2.0[10] | 2.0[10] |
| Cladding Thickness (m) | $8.6 \times 10^{-4}$ | $9.6 \times 10^{-4}$ |
| $A_o$ (m/h) | $2.97 \times 10^{-4}$ | $1.06 \times 10^{-4}$ |
| B (m) | $3.3 \times 10^{-5}$ | $3.3 \times 10^{-5}$ |
| C ($Pa^4\text{-}m\text{-}h$) | $8.21 \times 10^{6}$ | $1.69 \times 10^{7}$ |

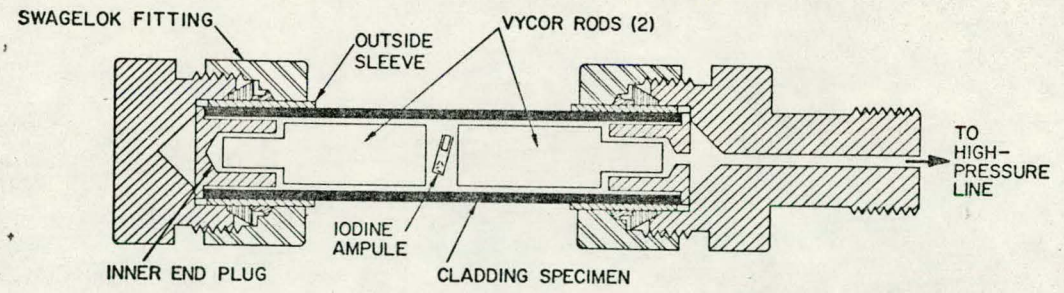


Fig. 1. Test Specimen Configuration.

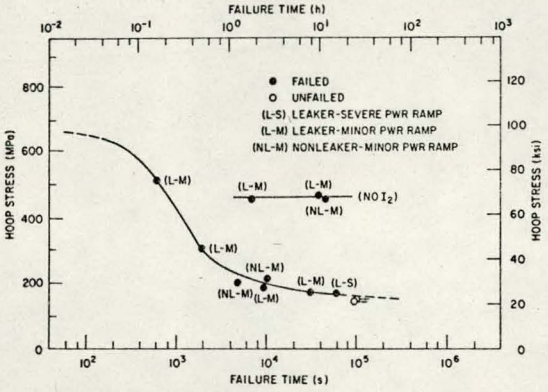


Fig. 2. SCC Test Results for OSK-1 Cladding (344°C).

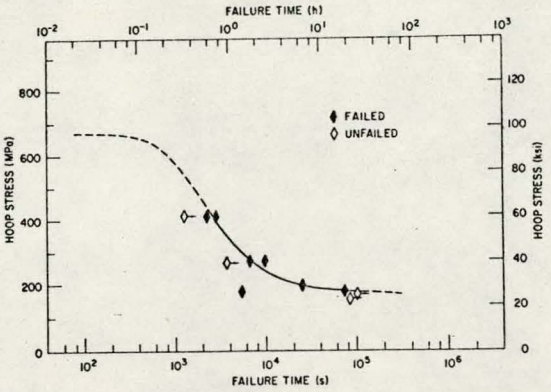


Fig. 3. SCC Test Results for QC Cladding (320°C).

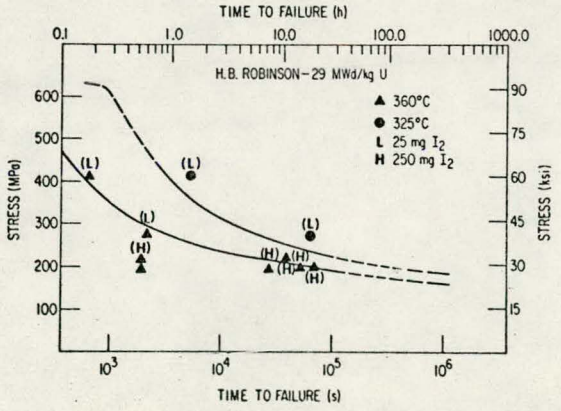


Fig. 4. SCC Test Results for HBR Cladding.

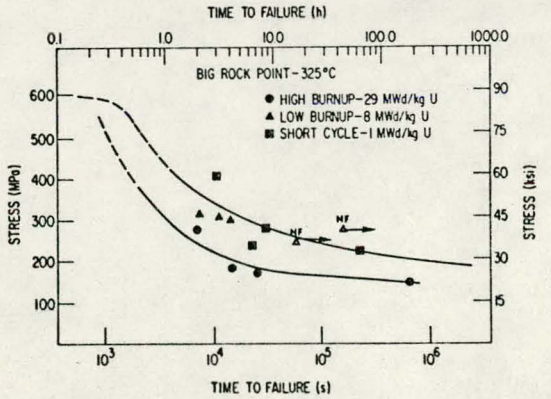


Fig. 5. SCC Test Results for BRP Cladding.

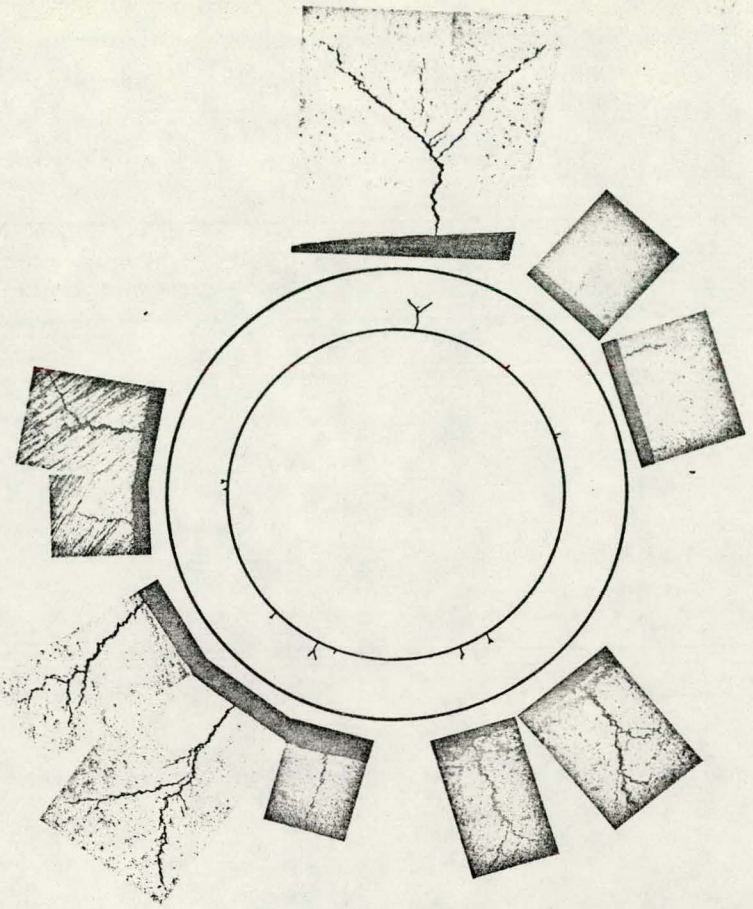

Fig. 6. SCC Cracks in Failed BRP (High-burnup) Cladding (Etched).

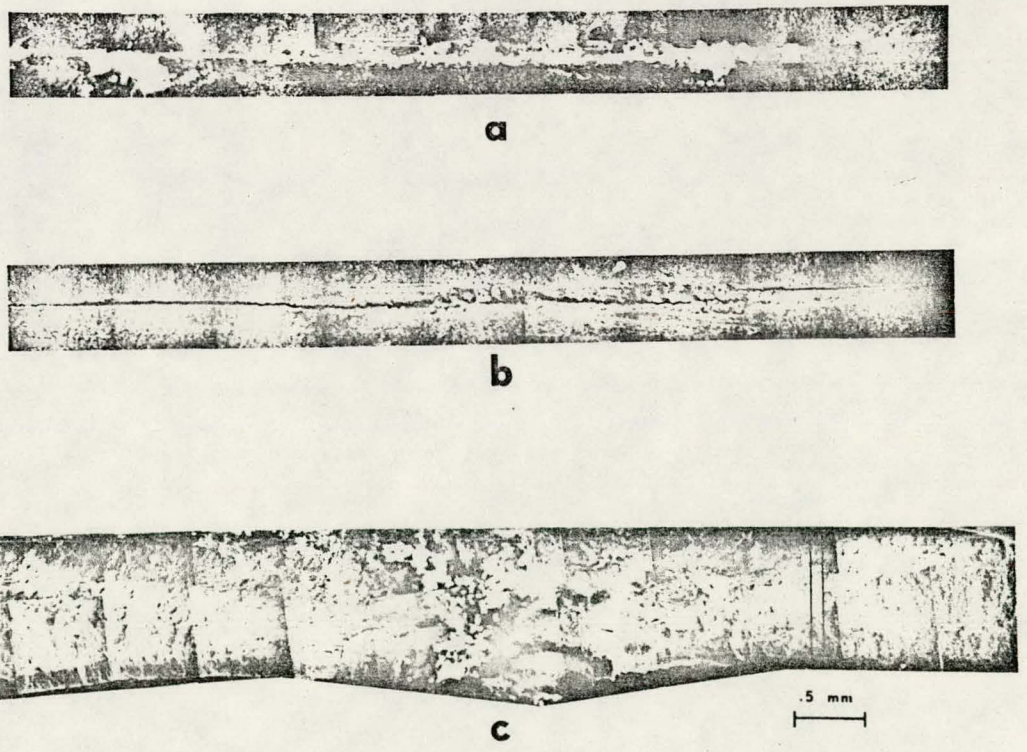


Fig. 7. Stress-corrosion. Crack on ID Surface of a QC Specimen. (a) As tested; (b) after ultrasonic cleaning; (c) after three-point bending to expose the fracture surface.

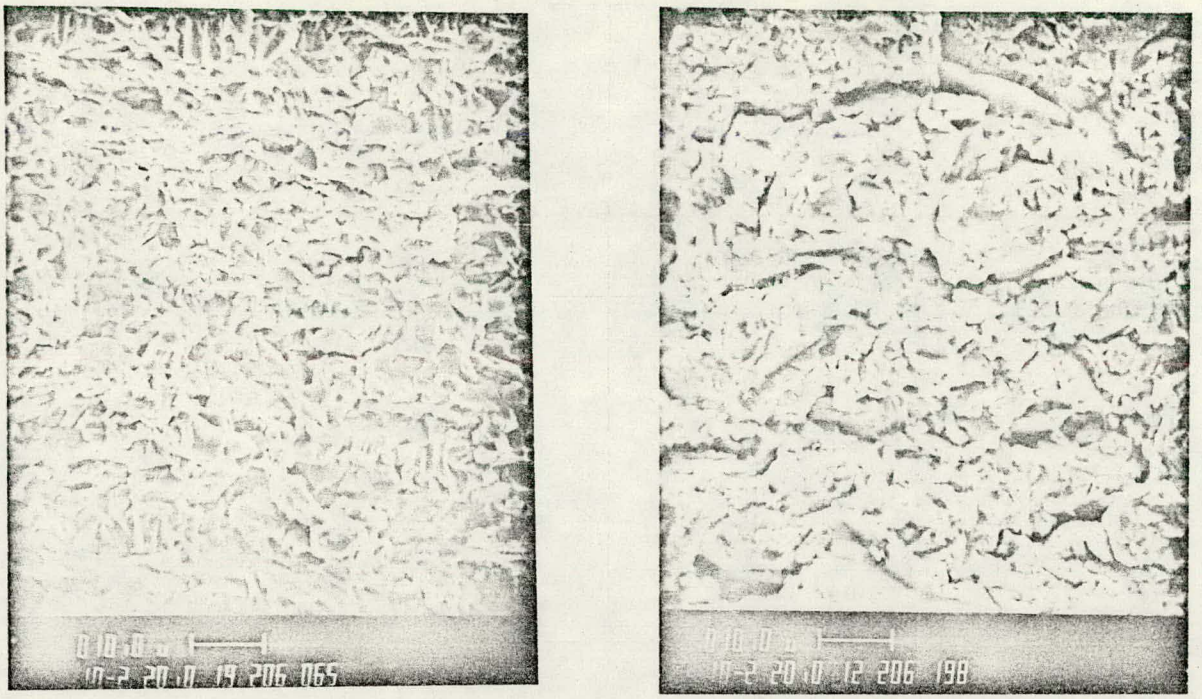

(a) (b)

Fig. 8. Fracture surfaces of QC specimens tested at (a) 182 MPa and (b) 412 MPa.

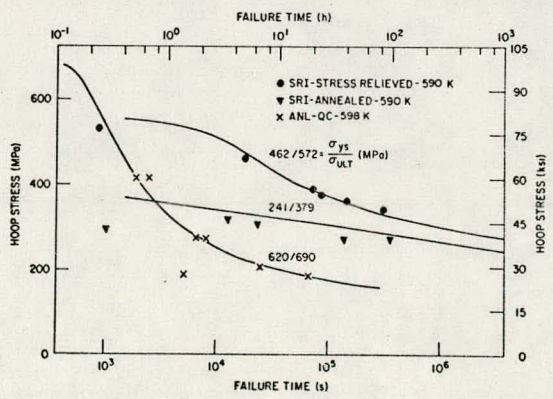


Fig. 9. Comparison of SCC Model Predictions and Iodine SCC Test Results.